The Performance Comparison of the Hybrid Solid Oxide Fuel Cell (SOFC) and Gas Turbine (GT) Systems

P. Chinda[1,*] *and P. Brault*[2]

[1]*Department of Mechanical Engineering Technology, College of Industrial Technology, King Mongkut's University of Technology North Bangkok, 1518, Piboonsongkram Road, Wong Sawang, Bangsue, Bangkok, 10800, Thailand*

[2]*Groupe de Recherches sur l'Energétique des Milieux Ionisés (GREMI), UMR 6606 CNRS-Université d'Orléans, BP6744, 45067, Orléans Cedex 2, France*

***Abstract*-- A hybrid solid oxide fuel cell and gas turbine system model is developed. The simple models are used in the preliminary part of the study and more realistic one based on the performance maps. Some important observations are made during the configuration study. The fuel cell performance is found to be a strong function of operating temperature. The parameters that limit the cycle performance are the SOFC temperature, the turbine inlet temperature, and the exhaust temperature. Though at high SOFC temperature, the cycle efficiency is high, the cycle operation under these conditions is not feasible after a certain point. The important fact found was that the selected configuration, at sea level conditions, a hybrid solid oxide fuel cell and gas turbine power system can achieve cycle system efficiency better than the reference. The results of the selected model were validated by comparing with reference cycle from literature.**

***Keywords* – Cycle, Efficiency, Gas Turbine, Hybrid, Performance Map, Sea Level, Solid Oxide Fuel Cell**

I. Nomenclature

A	total heat transfer area [m^{-2}]
C_c	heat capacity of the cold stream [$J.s^{-1}.K^{-1}$]
C_h	heat capacity of the hot stream [$J.s^{-1}.K^{-1}$]
C_{pa}	specific heat at constant pressure of air [$J.kg^{-1}.K^{-1}$]
C_{pg}	specific heat at constant pressure of combustion gases [$J.kg^{-1}.K^{-1}$]
C_{va}	specific heat at constant volume of air [$J.kg^{-1}.K^{-1}$]
C_{vg}	specific heat at constant volume of combustion gases [$J.kg^{-1}.K^{-1}$]
i_{cell}	single cell current density [$A.cm^{-2}$]
n_{cells}	the number of single cells required
P	pressure [atm]
P_C	mechanical power consumed by the compressor [Watt]
P_{MG}	mechanical power delivered to the generators [Watt]
P_{TG}	mechanical power delivered by the gas turbines [Watt]
q_{air}	air flow rate in [$kg.s^{-1}$][*]
T	temperature [K]
UA	the overall heat transfer coefficient [$W.K^{-1}$]
V_{bus}	bus voltage [Volt]
V_{cell}	single cell voltage [Volt]
γ_a	ratio of specific heat of air
γ_g	ratio of specific heats of combustion gases
η_C	efficiency of the compressor [%]
η_{TG}	efficiency of the turbine [%]
η_{trans}	transmission efficiency from turbine to compressor [%]
η_∞	polytropic efficiency of the turbine [%]
$\eta_{\infty C}$	polytropic efficiency of the compressor [%]
Δh_C	change in isentropic enthalpy of compressor [$J.mol^{-1}$]
Δh_{TG}	change in isentropic enthalpy of turbine [$J.mol^{-1}$]
ΔT_{lm}	log-Mean Temperature Difference (LMTD) [K]

Subscripts

DP	design point
e	exit
i	inlet

[*] Corresponding author: *penyaratc@kmutnb.ac.th,*

II. Introduction

To overcome the threats posed by climate change and energy security, advanced clean energy technologies are urgently needed. The solid oxide fuel cell (SOFC) power plant is known to be a potential alternative in the electric utility, for domestic, commercial and industrial sectors. It produces less harmful chemical and acoustic emissions at higher efficiency than the conventional technologies. Unlike the low-temperature polymer fuel cell, SOFC operates at temperatures high enough to enable the direct reformation of natural gas. SOFC converts the hydrogen, reformed from the natural gas, electrochemically producing both electrical power and high-grade waste heat for combined heat and power (CHP) system.

It has been demonstrated by simulation technique that SOFC can achieve 50% net electrical efficiencies and have already been considered feasible for integration with multi-MW gas turbine engines to achieve considerably high electrical efficiency [1]. Siemens-Westinghouse Power Corporation developed the first advanced power system, which integrates a SOFC stack with the gas turbine engines. The pressurized (3 atm) system generates 220 kW of electrical power at a net electrical efficiency of 55% [2]. Depending upon the application, different models are available in the open literature and there are large differences in the level of details in the models presented. Lumped models have been center of attention and have been largely used for studies of different cycle configurations [3, 4] and to some extent for part-load studies [5, 6] and [7]. As mentioned earlier, the great benefit of using lumped models is simplicity of the model development and short calculation time. A large amount of experimental data and mathematical relations exists for components such as compressors, turbines and heat exchangers, so these components can be modeled fairly accurately despite the lumped approach [8]. The lumped approach in SOFC models also facilitates uncomplicated changes between different geometries, as this only involves changes in geometry specific parameters. Accordingly, lumped models are also easier to adjust to experimental data. The disadvantage of lumped SOFC models is that they can only account for mean values of the parameters and it follows that more detailed investigation of the cell is needed to check for undesirable effects such as thermal cracking, coking or exceeding temperature limits locally [9]. This problem may be partly avoided by using a lumped model for system calculations, and a detailed model to test the validity of the results. Obviously, implementing a detailed SOFC model in the system model gives the most accurate results and this approach has been followed in [10].

In spite of the advantages of the SOFC-GT hybrid system, many technical barriers have to be overcome for the successful commercial development of this power generation technology. Therefore, design parameters need to be varied to determine performance sensitivity, and fundamental analysis is still needed to determine the practical operating conditions for most efficient operation. System modeling combined with thermodynamic optimization can be a valuable tool in technological research, providing indications of technical feasibility, identifying ways to improve efficiency, and determining the better configuration and conditions for an integrated power plant. In this work, the model is based on theoretical fundamentals and has been calibrated empirically. Based on the works in the previous study [7, 10], the author further develops the hybrid SOFC-GT power system model.

The emphasis of this study is to reduce the reliance on experimental data for plant performance prediction, and to extend the code developed previously for possible part load simulation in the future.

III. Modeling Of Sofc – Gas turbine Hybrid Systems

A gas turbine cycle is based on the Brayton cycle, which is a simple series of compression, combustion, and expansion processes. The main components of the cycle are a compressor, a combustor (combustion chamber), and a gas turbine. The number of components is not limited to three as the cycle may consist of several compressors and turbines (expanders). Figure 1 illustrates the basic schematic of a gas turbine engine. The ambient air is compressed and sent to the combustor. The constant pressure combustion takes place and the exhaust is sent to the turbine where power is extracted to drive the compressor and the generator. Heat exchangers can also be used to preheat the stream entering the combustion chamber.

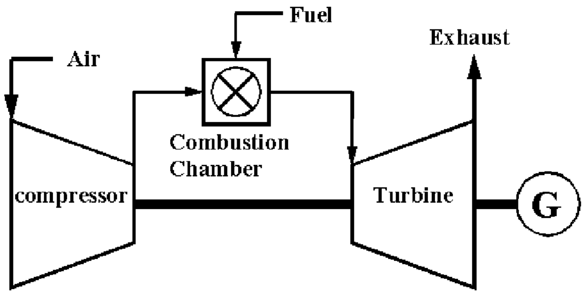

Fig. 1. Schematic of a gas turbine engine based upon the Brayton cycle

Gas turbine engines are generally used for power production falling in the range of few kilowatts to several megawatts and offer an electrical efficiency of 30 - 40%. This can be further improved by adding a topping cycle to achieve efficiencies of up to 60%. A gas turbine can be directly or indirectly connected to the SOFC. In an indirect integration, the combustor of the gas turbine is replaced with a heat exchanger in which air from the compressor is heated by the fuel cell exhaust and the SOFC can operate under atmospheric conditions. Although, it reduces the sealant requirement in the SOFC stack, the heat exchanger has to operate at very high temperatures and pressure differences. The material requirements in the indirect integration are really an issue and hence, it is not generally used. Figure 2 shows a direct integration of a solid oxide fuel cell and a gas turbine system. As can be seen from it, the combustion chamber of the gas turbine engine has been replaced with an SOFC and an afterburner. The pressurized stream from the compressor goes into the SOFC. The exhaust from the SOFC goes to the afterburner and the resulting high temperature and pressure exhaust enters into the turbine. In this case, the SOFC operates at high pressure, which further improves its performance. Moreover, heat exchangers are added after the turbine exhaust to further utilize the waste heat in preheating of the streams entering the SOFC stack. The high-pressure operation of SOFC stack causes large pressure gradients between anode and cathode. This pressure imbalance needs to be avoided, due the brittleness of the SOFC materials, and good sealants are required to stop leakages [11, 12].

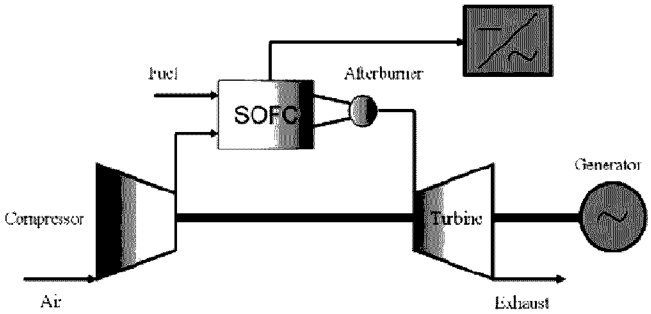

Fig. 2. Gas turbine engine as a bottoming cycle in a SOFC-gas turbine system [12]

The selecting a configuration is one of the key steps before designing a hybrid system. This present work aims for a commercial aircraft electrical power unit. The simple model is used in the preliminary step of the study and a more realistic one based on the performance maps is developed. A final necessary note is that future SOFC technology is projected for this application and specifically for this analysis. Systems analyses such as the following are required at this early stage and projections for both technology and the application are a challenging part of the design process. SOFC and SOFC-GT hybrid technology have made progress over the past decades but further maturity is necessary before an application such as this is feasible. Systems studies may extrapolate the capability of a technology, but the studies also quantify the necessary gains that must be made for feasibility. And the emphasis of this study is to reduce the reliance on experimental data for the performance prediction, and to extend the code developed previously for possible part-load simulation in the future. This topic presents various configurations of the SOFC – gas turbine hybrid system and discusses why one configuration is better than the other. Once the optimum configuration is selected, a complete cycle analysis is presented. The modeling equations are shown below.

A Solid oxide fuel cell modeling

A SOFC stack has been modeled using MATLAB [13]. The details of this model are presented in our previous works [14-18] and can be briefed that for this SOFC unit cell is a microscopic model based on the assumption that the electrodes were formed by spherical-shape particles and takes into account electronic, ionic, and gas transport together with the electrochemical reaction. It also considers the influence of the electrode structures on the electrochemical reaction at the three phase boundary (TPB). As mentioned earlier, the single cell model is extended into a stack model before creating a SOFC hybrid system. An operating point in figure 3 that is an example for a SOFC operates at 1073 K, 97% H_2 and 3 %H_2O, which shows the chosen voltage curve and the corresponding current density that are used to size the stack. Based on the given specifications (bus voltage, V_{bus} (volt)), the number of cells required (n_{cells}) can be calculated. In this work, a current density of 1 A.cm^{-2} was chosen for the SOFC operates at an average temperature of 1073 K and at the difference operating conditions, so the chosen current density is changed.

The number of single cells required (n_{cells}) to form the stack is computed as

$$n_{cells} = \frac{V_{bus}}{V_{cell}} \tag{1}$$

Where V_{cell} (volt) is single cell voltage.

Equation (1) assumes that the cells are arranged in series. Similarly, the area of each cell (A, cm^{-2}) within the stack can be calculated using the single cell current density (i_{cell} , A.cm^{-2}) and the stack current as shown in equation (2) :

$$A = \left(\frac{W_{max}}{V_{bus}}\right) \Big/ i_{cell} \tag{2}$$

Other components of the hybrid system like heat exchanger, compressor, gas turbine, and combustor have been modeled using the same simulation tool. All the components have been integrated to form a cogeneration power system and thermodynamics behavior the cycle that can be being studied.

B Component models

B.1 Compressor model

In the hybrid system, ambient air is compressed using the compressor and supplied to the SOFC. Model of the compressor is based on the perfect gas equations and polytropic transformations. Following equations have been used in compressor model:

The exhaust temperature:

$$T_e = T_i \left(\frac{p_e}{p_i}\right)^{(\gamma_a - 1)/\gamma_a \eta_{\infty c}} \tag{3}$$

Where, i - inlet, e - exit, P - pressure, T - Temperature

$\gamma_a = c_{pa}/c_{va}$ - Ratio of specific heats of air

η_{∞} - Polytropic efficiency of the compressor

Change in isentropic enthalpy:

$$\Delta h_C = C_{pa} T_i \left(\frac{P_e}{P_i}\right)^{R_a / C_{pa}} - 1 \tag{4}$$

Efficiency of the compressor:

$$\eta_C = \frac{1 - (p_e / p_i)^{\left(\frac{\gamma_a - 1}{\gamma_a}\right)}}{1 - (p_e / p_i)^{\left(\frac{\gamma_a - 1}{\gamma_a \eta_{\infty C}}\right)}} \tag{5}$$

Mechanical power consumed by the compressor:

$$P_C = \frac{q_{air} \Delta h_C}{\eta_C \eta_{trans}} \tag{6}$$

Where q_{air} - air flow rate in kg/s, η_{trans} - the transmission efficiency from turbine to compressor.

B.2 Turbine model

In the hybrid system, turbine is used to drive the compressor and as a secondary electrical power device. Turbine has been modeled in the same way as the compressor following equations model the gas turbine for a uniform polytropic expansion,

The exhaust temperature:

$$T_e = T_i \left(\frac{p_e}{p_i} \right)^{(\gamma_g - 1)/\gamma_g \eta_{\infty TG}} \tag{7}$$

Where, i - inlet, e - exit, P - pressure, T - Temperature

$\gamma_g = c_g / c_g$ - Ratio of specific heats of combustion gases

$\eta_{\infty TG}$ - Polytropic efficiency of the turbine

Change in isentropic enthalpy:

$$\Delta h_{TG} = C_{pg} T_i \left(\frac{p_e}{p_i} \right)^{R_g / C_{pg}} - 1 \tag{8}$$

Gas Turbine efficiency:

$$\eta_{TG} = \frac{1 - (p_e / p_i)^{\left(\frac{\gamma_a - 1}{\gamma_a \eta_{\infty TG}} \right)}}{1 - (p_e / p_i)^{\left(\frac{\gamma_g - 1}{\gamma_g} \right)}} \tag{9}$$

Now, the mechanical power delivered by the gas turbines can be calculated as:

$$P_{TG} = \eta_{TG} q_{TG} \Delta h_{TG} \tag{10}$$

And finally, mechanical power delivered to the Generators to produce electricity:

$$P_{MG} = P_{TG} - P_C \tag{11}$$

B.3 Heat exchanger model

Hybrid system is using parallel flow heat exchanger model. Following is the concept used to model the heat exchanger:

Where, C_h - heat capacity of the hot stream, C_c - heat capacity of the cold stream, U - overall heat transfer coefficient, A - total heat transfer area, ΔT_1 and ΔT_2 - stream to stream temperature differences in the front and back section of heat exchanger:

$$\Delta T_1 = T_{h,1} - T_{c,1} \tag{12}$$

$$\Delta T_2 = T_{h,2} - T_{c,2} \tag{13}$$

The proportionality between total heat transfer rate q and the overall thermal conductance of the heat exchanger surface is:

$$q = UA\Delta T_{lm} \tag{14}$$

Where ΔT_{lm} - the log mean temperature difference (LMTD) and defined as under:

$$\Delta T_{lm} = \frac{\Delta T_2 - \Delta T_1}{ln\left(\frac{\Delta T_2}{\Delta T_1} \right)} \tag{15}$$

and, $dq = -CdT$ gives streams exit temperatures once q is known. U is Overall heat transfer coefficient; A is Total heat transfer area.

B.4 Combustor model

The streams coming out of the fuel cell are combusted with additional fuel and air in the combustor and the high temperature exhaust is sent to turbine. Following equation models the flow in the combustor.

Enthalpy of Fuel Cell Streams + Enthalpy of additional fuel = Net Enthalpy of the mixture

$$dH = C_p\,(T)\,dT \tag{16}$$

Using the above equation and known mixture enthalpy,

$$\Delta h_C = C_{pa} T_i \left(\frac{p_e}{p_i} \right)^{R/C_{pa}} - 1 \tag{17}$$

Exhaust temperature is calculated. As of now, model assumes the complete combustion and there are no NO_x formed during the combustion.

C Configurations and cycles analysis

Deciding upon the optimum configuration is one of the key steps in modeling a gas turbine hybrid system. In this work, a few configurations of the hybrid system are simulated and their performances are analyzed. Based upon the comparative study, the better configuration is chosen and discussed in detail. The basic parameters that are focused at, in choosing the optimum configuration, are the cycle efficiency and the fuel cell power. The modeling assumptions, operating conditions and cycle configurations are shown below.

C.1 Modeling assumptions and operating conditions

Due to the solid oxide fuel cell and gas turbine hybrid system usually use as an auxiliary aerospace power. The models in this work aim for the aircraft applications. Sea level full power is taken as the design condition of the system. For aircraft applications, this choice is based upon the fact that the exhaust pressure at sea level is higher than the one at cruise altitude. In this way, the power extracted from the turbine will be less and to meet the power requirements the stack power needs to be higher. Higher stack power means higher heat and higher external cooling and thus higher air flow rate to the stack. Higher airflow rates require higher compressor power and higher turbine work. Therefore, the line of arguments suggests that sea level full power should be the design point. The fuel cell power is maximized at the design point. This design point selection and the operating conditions for the cycle components and reasoning are taken from [19].

• The operating conditions for the cycle components and the design point are:

Compressor pressure ratio: 2.88

Turbine Pressure ratio: 2.37

Fuel composition: 97% H2 + 3%H2O per mol

Air composition: 21% O2 + 79% N2 per mol

Design Temperature: 25 °C

Design Pressure: 1 atm

• For comparison the models assume that the cycles are running at design point until the optimum configuration is chosen.

• Pressures losses in the fuel cell, combustor, and piping are negligible.

• The combustor of the model is based on simple combustion reactions and does not include the actual chemistry of the reaction and the complete system is adiabatic i.e. no wall heat losses.

• Hydrogen is used as a fuel and hence internal reforming and desulphurization have not been incorporated.

C.2 The configurations

Initial numbers like SOFC power required, heat exchanger, turbine/compressor specifications etc are temporary numbers and have been assumed to get an idea how system performance depends upon the operating parameters. These numbers can be changed depending upon the system requirements. The first configuration has been chosen based upon the idea that since combustor exhaust is at high temperature, even the low mass flow rate will be enough to heat the fuel stream to a required temperature. The second configuration is the proposed configuration and the only difference is that here both (fuel and air) the streams are heated by the turbine exhaust. For both configurations are shown below.

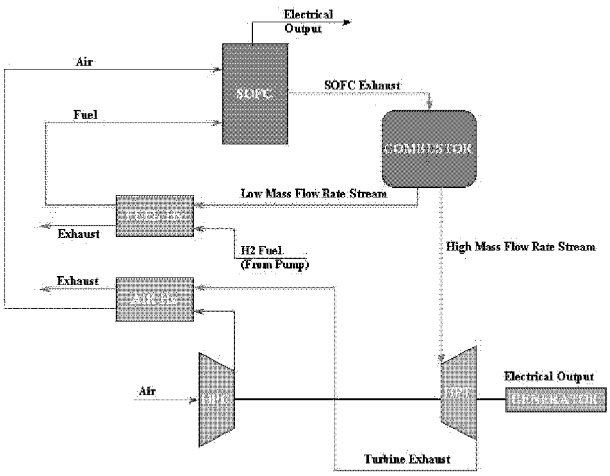

Fig. 3. Schematic of the first configuration

TABLE I
THE DATA AND DESIGN PERFORMANCE OF THE MODEL FOR THE FIRST CONFIGURATION

Efficiency	Com pressor	SOFC	Turbine	Combus tor	Fuel Hx	Air Hx
Power	68.5%	45%	88.4%	100 %	-	-
Temp Inlet	55.24 kW	198 kW (Elec)	120 kW (Mech)	-	-	-
Temp Outlet	298 K	1089 K Fuel 1086 K Air	1722 K	1155 K	1722 K 298 K	1292 K 462.7 K
Pressure Ratio	462.7 K	1155 K	1292	1722 K	1093 K (Exhaust)	1161K (Exhaust)
Fuel	4	1	0.3		-	-
Air	-	7.92 g/s	-	3.72 g/s	-	-

Table 1 shows the results of configuration 1. All the numbers shown below correspond to steady state. And table 2 shows the results of configuration 2. All the numbers shown below correspond to steady state too.

TABLE II
THE DATA AND DESIGN PERFORMANCE OF THE MODEL FOR THE SECOND CONFIGURATION

Efficiency	Com pressor	SOFC	Turbine	Combus tor	Fuel Hx	Air Hx
Power	68.5%	45%	88.4%	100 %	-	-
Temp Inlet	78.8 kW	198 kW (Elec)	205 kW (Mech)	-	-	-
Temp Outlet	298 K	1090 K Fuel 1091 K Air	1723 K	1159 K	1290 K 298 K	1290 K 462.7 K
Pressure Ratio	462.7 K	1159 K	1290	1723 K	1079 K (Exhaust)	1155 K (Exhaust)
Fuel	4	1	0.3		-	-
Air	-	4.2 g/s	-	5.86 g/s	-	-

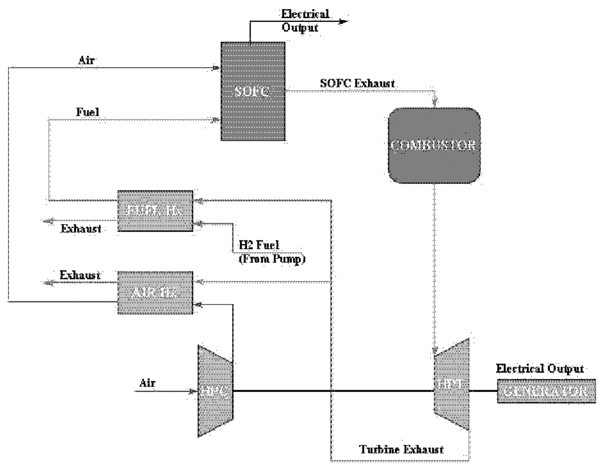

Fig. 4. Schematic of the second configuration

Given the turbine's maximum allowable inlet temperature (1750 K) and fixing other components specifications (like SOFC power and required inlet conditions and heat exchanger specifications) fixes the delivered mechanical output by the turbine. Since the turbine exhaust is at a lower temperature than the combustor exhaust and heating both the streams by turbine exhaust needs higher mass flow rates in the second case. High mass flow at turbine exit means higher fuel and airflow in the combustor and these high flow rates are reflected in terms of higher turbine power (205 kW) in the second case.

From the Table 3, it can be seen that configuration 1 has the lower performance than configuration 2 that gives the better steady state performance. Configuration 1 gives efficiency only about 42%. We can say that the low performance of configuration 1 can be attributed to the low operating temperature of the fuel cell stack, as the SOFC performance is directly proportional to the operating temperature. Also, the turbine inlet temperature is exceeding the maximum allowable temperature (1750 K). As we move from configuration 1 to 2, the operating temperature improves and hence the performance of the fuel cells.

The configuration 2 is chosen as the better configuration out of the configurations studied. Since not very high temperatures are required at the turbine exit, due to the high efficiency of the heat exchangers. The high temperature exhaust from the combustor is expanded in the turbine. The enthalpy of the exhaust leaving the turbine is high enough to give the required preheating to the air stream in the air heat exchanger. The exhaust from the air heat exchanger is released to the ambient. The efficiency obtained in this case is 58%. The turbine inlet temperature is also within the limits and exhaust temperature is lower than another configuration.

TABLE III
COMPARATIVE DATA AND RESULTS FOR THE TWO CONFIGURATIONS

	Configuration 1	Configuration 2
Fuel flow (g/s), SOFC	7.92 g/s	4.2 g/s
Fuel flow (g/s), combustor	3.72 g/s	5.86 g/s
Air flow (g/s), compressor	380 g/s	541.9 g/s
Air flow (g/s), SOFC	100 g/s	100 g/s
Air flow (g/s), combustor	280 g/s	441.9 g/s
SOFC average operating temperature (°C)	837	840.33
Turbine inlet temp (°C)	1722 K	1723 K
SOFC power (kW)	198 kW (Elec)	198 kW (Elec)
HPT (kW)	120 kW (Mech)	205 kW (Mech)
Total power (kW)	318	403
Cycle efficiency	42 %	58 %
Exhaust temp(°C), (fuel heat exchanger)	1093 K (Exhaust)	1079 K (Exhaust)
Exhaust Temp(°C), (air heat exchanger)	1161K (Exhaust)	1155 K (Exhaust)

C.3 Sensitivity study of configuration 2

Table 4 shows the data for configuration 2 at different mass flow rates for varying overall heat transfer coefficients (UA). 'Forbidden' means that a particular condition is not permissible as the maximum allowable turbine inlet temperature is 1750 K. As we move from low UA to high UA, the 'forbidden' operating condition shifts to the higher mass flow rates. An overall heat transfer coefficient of, UA, is used in configuration 2 with from [19].

TABLE IV
DATA FOR CONFIGURATION 2 FOR DIFFERENT HEAT TRANSFER COEFFICIENTS AND AIR MASS FLOW RATES

Heat exchanger overall heat transfer coefficient = 2000 w/m^{2}K					
Air flow (kg/s)	Stack temp. (K)	Cycle efficiency	Turbine inlet temp (K)	Exhaust temp (K)	Heat exchanger effectiveness %
0.4	1550	60	1959 (forbidden)	851	92
0.45	1364	61.2	1764 (forbidden)	777	90
0.5	1210	60.7	1599	720	87.4
0.55	1084	56.2	1462	677	85
0.6	983.8	47	1348	643	82.6
0.65	901	35	1253	617	80.5
0.7	834	14	1173	598	78.5
Heat exchanger overall heat transfer coefficient = 3000 w/m^{2}K					
Air flow (kg/s)	Stack temp. (K)	Cycle efficiency	Turbine inlet temp (K)	Exhaust temp (K)	Heat exchanger effectiveness %
0.4	Forbidden				
0.45					
0.5					
0.55	1247	62.5	1601	684	92
0.6	1129	60	1473	645.4	90
0.65	1030	53.2	1365	615	88.2
0.7	948	43.5	1272	591.5	86.5
Heat exchanger overall heat transfer coefficient = 4000 w/m^{2}K					
Air flow (kg/s)	Stack temp. (K)	Cycle efficiency	Turbine inlet temp (K)	Exhaust temp (K)	Heat exchanger effectiveness %
0.4	Forbidden				
0.45					
0.5					
0.55					
0.6	1230	63.2	1560	650	94
0.65	1124	60.5	1445	617	92.5
0.7	1033	54.2	1346	590	91
Heat exchanger overall heat transfer coefficient = 5000 w/m^{2}K					
Air flow(kg/s)	Stack temp. (K)	Cycle efficiency	Turbine inlet temp (K)	Exhaust temp (K)	Heat exchanger effectiveness %
0.4					
0.45					
0.5					
0.55					
0.6	1297	64.4	1618	654.4	96.3
0.65	1190	63.3	1503	619.5	95.2
0.7	1096	59.8	1401	591.5	93.9

D Improved configuration 2 design performance and comparison with the reference case

D.1 Improved configuration 2 design performance

From the previous analysis we have fixed the configuration and the components specifications. So far configuration 2 is based on the simplified compressor and turbine models. The models are now modified to include turbine and compressor maps. The improved model of configuration 2 uses performance maps for a real compressor (DLR radial) and turbine (NASA-CR-174646).

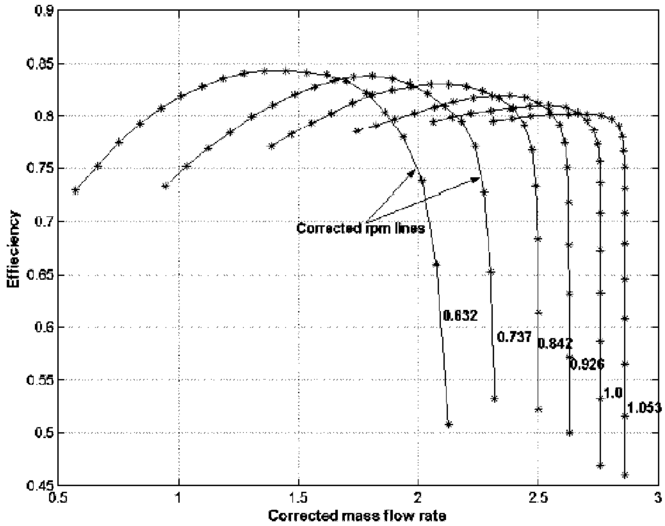

Fig. 5. Performance maps of the modeled compressor, based on the DLR radial compressor map (a) the relation between the corrected mass flow rate and efficiency

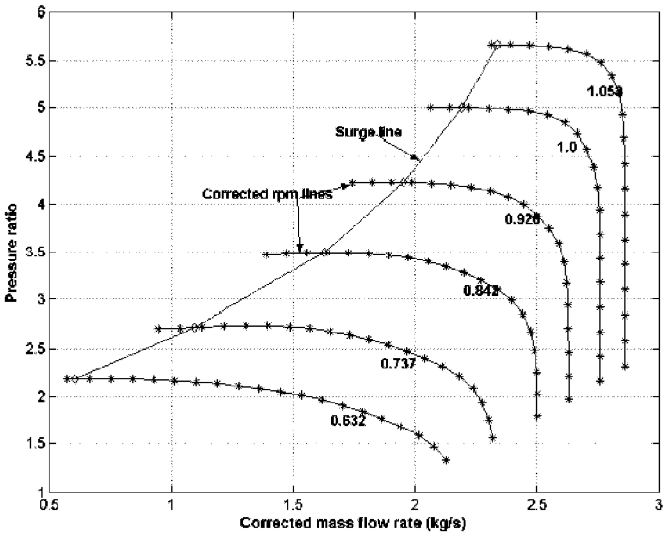

Fig. 5. Performance maps of the modeled compressor, based on the DLR radial compressor map (b) the relation between the corrected mass flow rate and pressure ratio

A compressor is generally designed for a basic set of delivery pressure, temperature, isentropic efficiency, and mass flow rate. These parameters depend upon the shaft speed, inlet temperature, pressure, and thermodynamic properties of the gas. When the compressor operates under this condition, it is often referred as design point operation. Operation under any other condition is referred to as off-design operation. Experimental results from off-design operation are often summarized in performance maps, in which the number of free variables is reduced by use of non-dimensional parameters for better readability. Dimensional analysis shows that constant corrected speed lines (Equation 18) can be plotted in two charts with corrected flow rate (Equation 20) on the x-axis, and with isentropic efficiency *(η)* or pressure ratio (π, Equation 19) on the y-axis. In Equations 18 to 20 the subscripts 01 and 02 relate to the stagnation values at the entry and exit, respectively. T and are the reference temperature and pressure. The performance map for the modeled radial compressor, based on [20], is shown in Figure 5.

$$N_{corr} = \frac{N}{\sqrt{T_{01}/T_a}} \tag{18}$$

$$\pi = \frac{P_{02}}{P_{01}} \tag{19}$$

$$\dot{m}_{corr} = \frac{m\sqrt{T_{01}/T_a}}{P_{01}/P_a} \tag{20}$$

The line in the bottom map of Figure 5 (Figure 5b), connects all the constant rpm lines and is called the surge line. Operation above this line may cause the compressor to surge and performance breakdown. Surge in a compressor occurs when there is insufficient mass flow or there is an aerodynamic stall in the initial stages of the compressor. In such cases, there is a complete break down of the flow field in the entire system and rapid changes in the mass flow lead to alternating stall and unstall behavior resulting in violent oscillations in pressure, propagation of pressure waves, and failure of the entire compression system.

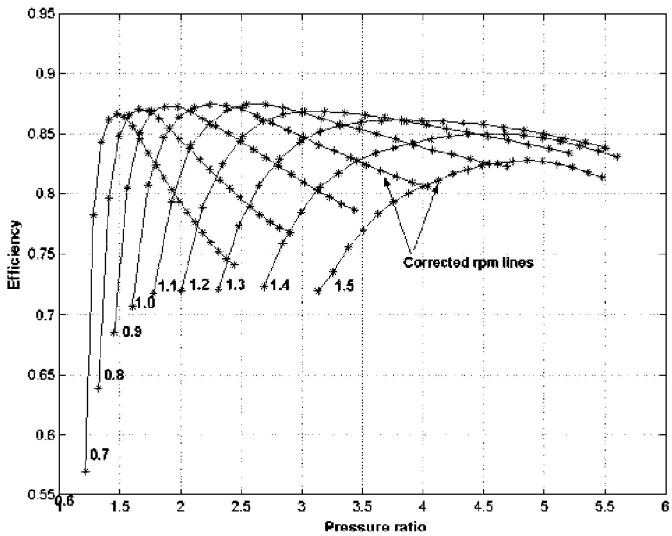

Fig. 6. Performance map of the modeled turbine, based on the radial turbine map NASA-CR-174646 (a) the relation between the pressure ratio and efficiency

A turbine is generally choked while operating near the design point. The exit stream properties can be calculated from the choked flow condition using equation 21.

$$\frac{\dot{m}}{\dot{m}_{DP}} = \frac{P_i}{P_e}\sqrt{\frac{1-\left(\frac{P_e}{P_i}\right)^2}{1-\left(\frac{P_e}{P_i}\right)^2_{DP}}} \qquad (21)$$

Where the subscript 'DP', 'i', 'e' represent the design point, inlet and outlet of the turbine, respectively. Figure 6 shows the generic performance map of the radial turbine used in the present modeling. The experimental data for the radial turbine is taken from the Kurzke's "Map Collection 2" referred to as NASA-CR-174646 [20]. As it can be seen from the generic maps, the turbine has a very large operation range in the choked condition. However, if the pressure ratio is low, the chocked assumption is no longer valid, and performance maps are required.

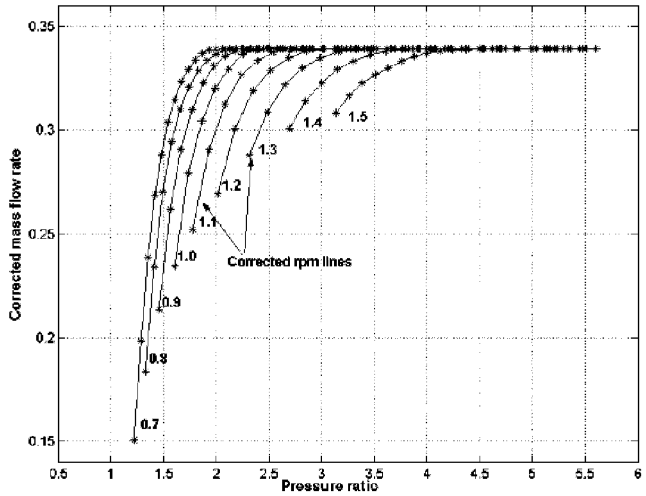

Fig. 6. Performance map of the modeled turbine, based on the radial turbine map NASA-CR-174646 (b) the relation between the pressure ratio and corrected mass flow rate

D.2 Comparison with the reference case

To calculate the design performance of the configuration, a steady state model of the SOFC is developed. One more difference between base configuration 2 and its improved version is that in the latter configuration, the turbine is split into a driving and a power turbine. The reason being that the compressor and the driving turbine need to be matched. One important point to be noted is that the analysis henceforth will use some adjustable parameters (compressor mass flow rate, pressure ratio) in order to simulate the same conditions as [19]. The parameters used for comparison are:

Compressor: DLR radial
Inlet temperature: 298 K
Inlet pressure: 101325 Pa
Design mass flow rate: adjustable
Design pressure ratio: 2.88
Air heat exchanger: Counter flow with an overall heat transfer coefficient (UA): 7000 w/m^{2}K
Fuel heat exchanger: Counter flow with an overall heat Transfer coefficient (UA): 360 w/m^{2}K
Power Turbine: NASA-CR-174646
Design mass flow rate: adjustable
Design pressure ratio: 2

Table 5 shows the results of improved of configuration 2 and the reference cycle [19]. The parameters shown in ***bold and italics*** are adjustable parameters and are varied in the model in order to compare the performance with the reference case.

TABLE V
DESIGN PERFORMANCE OF THE MODEL AND THE REFERENCE [19]

	Configuration 2	**Reference cycle [14]**
SOFC net power	**315 kW**	**429 kW**
Turbine power	**138 kW(mechanical)**	**19 kW(electrical)**
Cycle efficiency	**56.5%**	**42%**
Stack pressure	***2.9 bar***	***2.9 bar***
Stack temperature	***856 ºC***	***850 ºC***
Compressor inlet pressure	***14.7 psia***	***14.7 psia***
Compressor pressure ratio	***2.88***	***2.88***
Compressor efficiency	**85%**	**83%**
Turbine outlet pressure	***17.1 psia***	***17.1psia***
Turbine Pressure ratio	**2.47**	**2.37**
Turbine efficiency	**87%**	**84%**

The results show that the model is giving better sea level performance than the reference cycle [19]. The efficiency observed for the model is 56.5%, which is 14.5% more than the reference case.

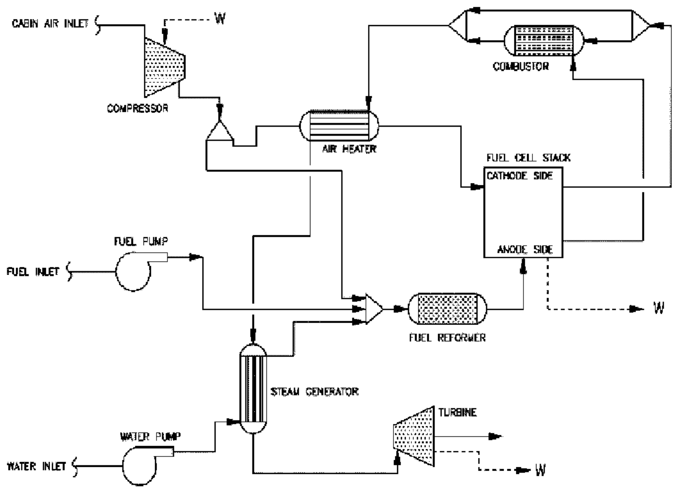

Fig. 7. ASPEN model of SOFC-GT hybrid system by NASA Glenn Research Center [19 ; reference cycle]

E Conclusion

A hybrid solid oxide fuel cell and gas turbine power system model is developed and implemented. Two types of models have been developed for compressors and turbines based on simple thermodynamic expressions. The simple models are used in the preliminary part of the study and a more realistic one based on the performance maps. Some important observations are made during the configuration study. Those are made by means of a sensitivity study of the whole cycle for the selected configuration. The fuel cell performance is found to be a strong function of operating temperature. The parameters that limit the cycle performance are the SOFC temperature, the turbine inlet temperature, and the exhaust temperature. Though at high SOFC temperatures, the cycle efficiency is high, the cycle operation under these conditions is not feasible after a certain point. The important fact found was that the selected configuration (configuration 2), at sea level conditions, a hybrid solid oxide fuel cell and gas turbine power system can achieve cycle system efficiency better than the reference cycle. The results of the presented model (configuration 2) were validated by comparing with the reference cycle results from the available literatures.

F Further work

Now, we can go through each of the previous mentioned assumptions one by one. The first assumption is that the system assumes no pressure loss anywhere which can be considered a reasonable assumption for preliminary modeling but there are many factors which contribute to the system pressure loss such as losses in the piping due to surface roughness, losses in the flow channels of the fuel cell and combustion losses. All of these losses can be approximately accounted for by doing the statistical study of the available literature. The entire analysis has been done for hydrogen fuel but in practical cases another hydrocarbon fuel can be used. In order to modify the system for the other hydrocarbon fuel, an internal reformer and a desulphurizer needs to be integrated with the system simulating the entire chemistry of the reactions taking place. The suggested for modeling the chemical reactions has been mentioned in the model. And the last assumption is that the combustor used in the system is based on simple combustion reactions and might not be actually simulating the chemical reactions occurring at the high operating temperatures. The model suggested that the chemical reactions of the combustor should be included in the model. Currently, the individual components of the system (compressor, turbine, heat exchanger and combustor) are modeled based upon the simple thermodynamic relations and assume the design point operation for the entire transient analysis, which is not the case in real life. So once the current design is complete and results are verified with the data available, dynamic analysis of each of the components and the cycle as a whole will be carried out and validated. The above discussion shows that modeling a hybrid system is an iterative process and has to be tested and retested before it can come close to a real system.

IV. References

[1] A.F. Massardo, and F. Lubelli, "Internal reforming solid oxide fuel cell - gas turbine combined cycles (IRSOFC-GT): part A - cell model and cycle thermodynamic analysis," *J. Eng. Gas Turbines Power,* vol. 122, pp. 27-35, 2000.

[2] J.H. Hirschenhofer, D.B. Stauler, R.R. Engleman, and M.G. Klett, *Fuel Cell Handbook*, (4th ed.) Parsons Corporation Reading P.A. for U.S. Department of Energy, 1998.

[3] W. Winkler, and L. Hagen, "Layout of SOFC-GT cycles with electric efficiencies over 80%", presented at the 4th European Fuel Cell Forum, Lucerne, Switzerland, 1-5 July, 2000.

[4] A.D. Rao, and G. S. Samuelsen, "A thermodynamic analysis of tubular SOFC based hybrid systems" presented at the ASME Turbo Exposition 2001, New Orleans, Louisiana, U.S.A., 4-7 June, 2001.

[5] S. Campanari, "Full load and part-load performance prediction for integrated SOFC and microturbine systems," *J. Eng. Gas Turbines Power*, vol. 122, pp. 239 – 246, 2000.

[6] P. Costamagna, L. Magistri, and A.F. Massardo, "Design and part-load performance of a hybrid system based on a solid oxide fuel cell reactor and a micro gas turbine," *J. Power Sources*, vol. 96, pp. 352 – 368, 2001.

[7] S.H. Chan, H.K. Ho, and Y. Tian, "Modeling of a simple hybrid solid oxide fuel cell - gas turbine power plant," *J. Power Sources*, vol. 109, pp. 111 – 120, 2002.

[8] D. Umberto, L. Gheorghe, Z. Dario, and L. Cristian, "A MATLAB - simulink analysis of hybrid SOFC dynamic behavior" presented at International Conference on Fuel Cell Science, Engineering and Technology, Ypsilanti, Michigan, U.S.A., 23-25 May, 2005.

[9] L. Magistri, R. Bozzo, P. Costamagna, and A. F. Massardo, "Simplified versus detailed SOFC reactor models and influence on the simulation of the design point performance of hybrid systems" presented at the ASME Turbo Exposition 2002, Amsterdam, The Netherlands.,3-6 June, 2002.

[10] J. Palsson, A. Selimovic and L. Sjunnesson, "Combined solid oxide fuel cell and gas turbine systems for efficient power and heat generation" *J. Power Sources*, vol. 86, pp. 442 - 448, 2000.

[11] J. Larminie and A. Dicks, *Fuel Cell Systems Explained*, New York: John Wiley & Sons Ltd, 2000.

[12] B. Thorud, "Dynamic modeling and characterization of a solid oxide fuel cell integrated in a gas turbine cycle," Ph.D. dissertation, Dept. Energy and Process Engineering. Eng., Univ. Norwegian University of Science and Technology, 2005.

[13] A. Gilat and V. Subramaniam, *Numerical Methods for Engineers and Scientists: an Introduction with Applications Using MATLAB*, (1st ed.) New York: John Wiley & Sons, 2008.

[14] P. Chinda, W. Wechsatol, S. Chanchaona, and P. Brault, "Microscale modeling of an anode-supported planar solid oxide fuel cell," *Fuel Cells*, vol. 11(2), pp. 184-199, 2011.

[15] P. Chinda, S. Chanchaona, P. Brault, and W. Wechsatol, "A planar anode-supported solid oxide fuel cell model with internal reforming of natural gas," *Eur Phys J Appl. Phys*, vol. 54(2), pp. 23405 - 1-15, 2011.

[16] P. Chinda, S. Chanchaona, P. Brault, and W. Wechsatol, "A solid oxide fuel cell micro-scale modeling with spherical particle shaped electrodes," *Eur Phys J Appl. Phys*, vol. 54(2), pp. 23411-1-16, 2011.

[17] P. Chinda, S. Chanchaona, P. Brault, and W. Wechsatol, "Mathematical modeling of a solid oxide fuel cell with nearly spherical-shaped electrode particles," *J. Sustainable Energy and Environment*, vol. 1(4), pp. 185-196, 2010.

[18] P. Chinda, W. Wechsatol and J.C. Ordonez, "Micro-scale modeling of a solid oxide fuel cell packed with spherical-shaped electrode particles" presented at the 3rd International Conference on Sustainable Energy and Environment (SEE 2009), Bangkok, Thailand, 19-22 May, 2009.

[19] J.E. Freeh, C.J. Steffen, and L.M. Larosiliere, "Off - design performance analysis of a solid oxide fuel cell - gas turbine hybrid for auxiliary aerospace power", in *Proc. FUELCELL2005 3rd International Conference on Fuel Cell Science Engineering and Technology*., pp. 74099-1-8.

[20] J. Kurzke, *Compressor and Turbine Maps for Gas Turbine Performance Computer Programs - Component Map Collection 2*, Joachim Kurzke, Dachau, 2004.

V. Biographies

Penyarat CHINDA was born in Samutsakhon, Thailand, on January 12, 1977. She graduated in bachelor, master and doctor of mechanical engineering from King Mongkut's University of Technology Thonburi (KMUTT), Bangkok Thailand. She received honorary scholarship from the

Thailand Higher Education Commission Fund and Graduated Student Diamond Scholarship from King Mongkut's University of Technology Thonburi for study in doctoral degree. She is a lecturer at Department of Mechanical Engineering Siam University between 2002 to 2006. Now, she is a lecturer at Department of Mechanical Engineering Technology, College of Industrial Technology, King Mongkut's University of Technology North Bangkok (KMUTNB), Bangkok, Thailand since after her graduation in doctoral degree in 2011. Her special fields of interest include in hydrogen energy, transport phenomena in fuel cell systems, fuel cells development and modeling.

Pascal BRAULT was born in LE BLANC, France, on February 15, 1961. He graduated Doctor of Philosophy in Plasma Surface Interactions from University of Orléans, Orléans, France. His employment experience included project manager in CNRS Energy Program (PLASMAPAC), Scientific manager of a large regional program on fuel cells involving European Social Fund (2 M€), Regional partner of the INTERREG IIIC "International Cooperation Platform for Sustainability", ICOPS project (www.icops.eu), Manager of the project "Future Energies" French government, Region Centre Project Contract (5 M€), Manager of Regional project on solid oxide fuel cell (300 k€), Referee for EU-ISTU projects (FP6), Referee for PHC program (France), Referee for numerous peer reviewed international scientific journal, Member of the scientific committee of the international conference, Innovations on Thin Films Processing and Characterisation. Pascal received honorary prize "Alexander von Humboldt Fellow 1992-1993", Max Planck Institute for Fluid Mechanics, Prof. J. P. Toennies, Göttingen Molecular beam interactions with metallic surfaces, and, Laureate of "Tremplin Recherche" , Prize from French Senate (12 february 2008). He is a Director of Recherche 2° Classe CNRS and Director of Laboratory FR776 EPEE, Energie, Propulsion, Espace, Environnement since January, 1st 2006 at Groupe de Recherches sur l' Energétique des Milieux Ionisés (GREMI) CNRS-Université d'Orléans, Orléans , France.